Supporting Information

Wenjuan Li,[a,b,#] Qi Shen,[a,#] Dandan Men,[b] Yujie Sun,[a] Wenwen Cao,[a] Jin Yong Lee,[e] Baotao Kang[a],* Yiqiang Sun[a,c,d,*] Cuncheng Li[a,*]

a School of Chemistry and Chemical Engineering, University of Jinan, Jinan 250022, China

b Jiangxi Key Laboratory of Surface Engineering, Jiangxi Science and Technology Normal University, Nanchang, 330013, P. R. China

c School of Materials Science And Engineering, University of Jinan, Jinan 250022, China

d Foshan (Southern China) Institute for New Materials, Foshan 528200, Guangdong, China

e Department of Chemistry, Sungkyunkwan University, Suwon, 16419, Republic of Korea

----

Experimental Section

Reagents. Cobalt nitrate ($Co(NO_3)_2 \cdot 6H_2O$), Ammonia fluoride (NH_4F), Urea (CH_4N_2O) , Ammonia solution ($NH_3 \cdot H_2O$), Dopamine hydrochloride ($C_8H_{11}NO_2 \cdot HCl$), Ethanol (CH_3CH_2OH), Selenium were purchased from Sinopharm group and used without further purification in all process. Deionized (DI) water used in all process were prepared with Milli-Q water with the resistance of 18 MΩ·cm at 25 °C.

Synthesis of $Co_2(OH)_2CO_3$ nanowires. In a typical process for the synthesis of synthesis of $Co_2(OH)_2CO_3$ nanowires, 1.6mmol $Co(NO_3)_2 \cdot 6H_2O$, 10mmol CH_4N_2O and 4mmol NH_4F were dissolved in 40 mL distilled water and stirred for 15 min to form a homogeneous solution. Then, the solution was transferred into a 50 ml Teflon-lined stainless-steel autoclave, which was sealed and kept at 120 °C for 6 h. After cooling to room temperature naturally, the products were washed via DI water several times, and then dried at 60 °C overnight.

Synthesis of $Co_2(OH)_2CO_3$@PDA nanowires. $Co_2(OH)_2CO_3$@PDA nanowires was obtained by a simple oil bath using $Co_2(OH)_2CO_3$ nanowires as the precursor. Under the condition of oil bath at 50 ℃ , 25 mg of the dried $Co_2(OH)_2CO_3$ nanowires precursor was placed in a round-bottom flask containing 25 ml of absolute ethanol, add 300 μL of ammonia solution with stirring. After 15 minutes of reaction, add 120 μL of 0.1 mol/L dopamine hydrochloride aqueous solution, continue to stir and react for 3 hours. After the reaction, the products were washed via DI water several times, and then dried at 60 °C overnight.

Synthesis of $CoSe_2$@N-C nanowires. The $CoSe_2$@N-C nanowires were obtained via a simple annealing strategy using $Co_2(OH)_2CO_3$@PDA nanowires as the precursor. In

the process of annealing, 100 mg of selenium powder and 25 mg the obtained $Co_2(OH)_2CO_3$@PDA nanowires were put at two separate positions in a porcelain boat with selenium powder at the upstream side of the furnace. After flushed with Ar, the furnace was heated to 400 °C for 90 min with a rate of 5 °C/min. After the reaction, the products of $CoSe_2$ nanowires coated with N-doped graphitized carbon were collected for further testing.

Electrochemical Measurements. All the electrochemical catalytic measurements were performed with a CHI 760E electrochemistry workstation (CH Instruments, Inc., Shanghai) in a standard three-electrode system. A conventional one-component three-electrode cell was used. The $CoSe_2$@N-C was used as the working electrode, an Ag/AgCl electrode was used as the reference electrode, and Carbon rod was used as the counter electrode. The electrocatalytic activity of the catalysts was examined via linear-sweep voltammetry in a N_2-purged 1 M KOH solution at 298 K and a scan rate of 5 mV s^{-1}. All potentials and voltages were IR corrected no otherwise specified. The electrochemical impedance spectroscopy (EIS) was obtained in the range of 100000 to 1 Hz at an amplitude of 5 mV. Cyclic voltammograms (CV) were measured from 1.3 to 2.8 V (vs. RHE) at scan rates of 5 mV s^{-1}. To prepare $CoSe_2$@N-C working electrode, 10 mg of the as-prepared catalysts and 43 μL 5 wt% Nafion solutions were dispersed in 250 μL ethanol and 250 μL deionized water with the assistance of ultrasonication to form a homogeneous catalyst ink. Then, each time take 52 μL catalyst ink drops on geometric surface area of the carbon cloth is 1cm × 1cm, repeat drips twice. Afterwards, let it evaporate in the air. The other control samples were also

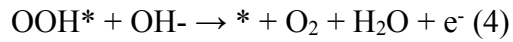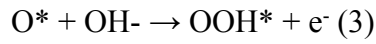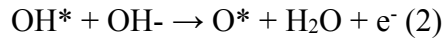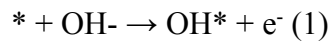synthetized, under otherwise identical conditions, except for using different materials. The mass loading of the materials in the electrode was approximately 1.915 mg cm^{-2}.

Characterizations. TEM (JEOL, JEOL-1400, 2100F 200 kV) were used to characterize the morphologies and structures of the samples. The X-ray diffraction (XRD) measurement was performed on a Philips X'pert Pro X-ray diffractometer with Cu K α radiation (λ=0.15419 nm). X-ray photoelectron spectroscopy (XPS) measurements were conducted on SPECS Phoibos 100 spectrometer. The specific surface area was measured on a Micromeritics TriStar II 3020 instrument according to the Brunauer-Emmett-Teller (BET) method.

Density Functional Theory Calculation. The exposed (200) surface of CoSe$_2$@N-C and CoSe$_2$ were selected for theoretical investigation due to the usual observation and stability in experimental studies. The CoSe$_2$ (200) and its composite with N-doped cabon (CoSe$_2$@N-C) were simulated as the OER catalysts. A C$_{27}$N$_3$H$_{14}$ complex was simulated as N-doped cabon for simplification. The lattice parameter in the Z direction was fixed with a vacuum space of 15 Å to avoid interlayer interaction. Then, OH, O, and OOH groups were absorbed at Co atom on the surface of these materials. The first-principles calculations in the framework of density functional theory, including structural, electronic performances, were carried out based on the Vienna Ab-initio Simulation Package known as VASP. The exchange correlation functional under the generalized gradient approximation with ultrasoft pseudopotentials and the Perdew Burke Ernzerh of functional was adopted to describe the electron electron interaction. In addition, for accurately describing the Coulomb correlation effect for

Co atom, which has 3d electrons, the PBE + U method within U = 3.40 eV (U is the on-site coulomb parameter) was also included. An energy cutoff of 450 eV was used and a k-point sampling set of $3 \times 3 \times 1$ was tested for convergence. All the atomic structures were fully optimized until all forces on each atom were smaller than 0.001 eV/Å.

In an alkaline medium, the electrochemical model of OER can be divided into four one-electron reactions:

$* + OH- \rightarrow OH* + e^-$ (1)

$OH* + OH- \rightarrow O* + H_2O + e^-$ (2)

$O* + OH- \rightarrow OOH* + e^-$ (3)

$OOH* + OH- \rightarrow * + O_2 + H_2O + e^-$ (4)

The free energy change of the reaction ΔG was calculated as the difference between the free energies of the initial and final states as shown below:

$\triangle G = \triangle E + \triangle EZPE - T\triangle S - eU$ (5)

where $\triangle E$ denotes the adsorption energy, $\triangle EZPE$ and $\triangle S$ respectively represent the changes of zero-point energy and entropy, T was set to 298 K, U is the potential at the electrode, and e is the transferred charge for single-electron reactions and was set to 1.

The overpotential (η) of OER can be evaluated from the Gibbs free energy differences of each step as:

$\eta^{OER} = max(\triangle G_1, \triangle G_2, \triangle G_3, \triangle G_4) / e - 1.23$ V (6)

where $\triangle G_1$, $\triangle G_2$, $\triangle G_3$, and $\triangle G_4$ are the free energy of reactions (1-4).
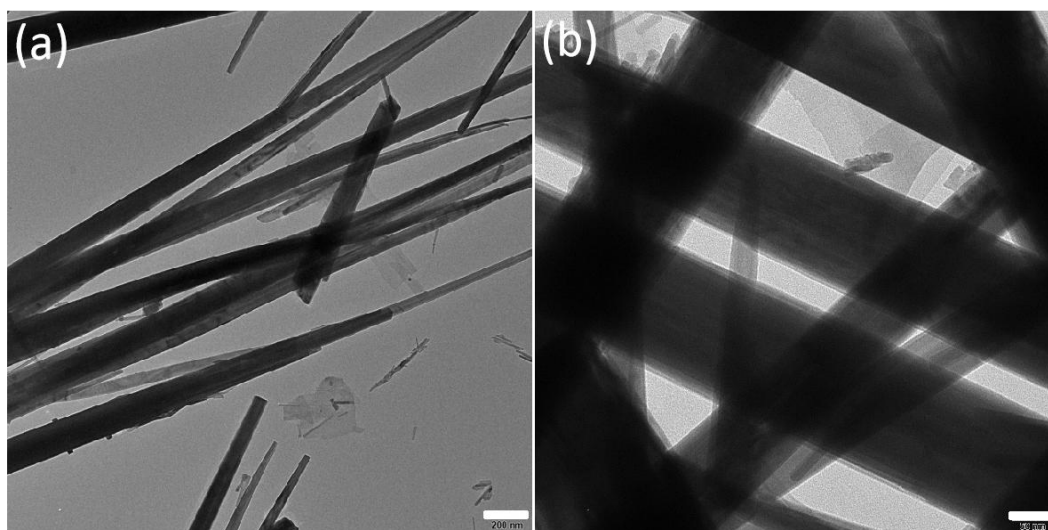
More supplementary figures:

Figure S1. (a) Low-magnification and (b) high-magnification TEM images of $Co_2(OH)_2CO_3$ nanowire precursor.

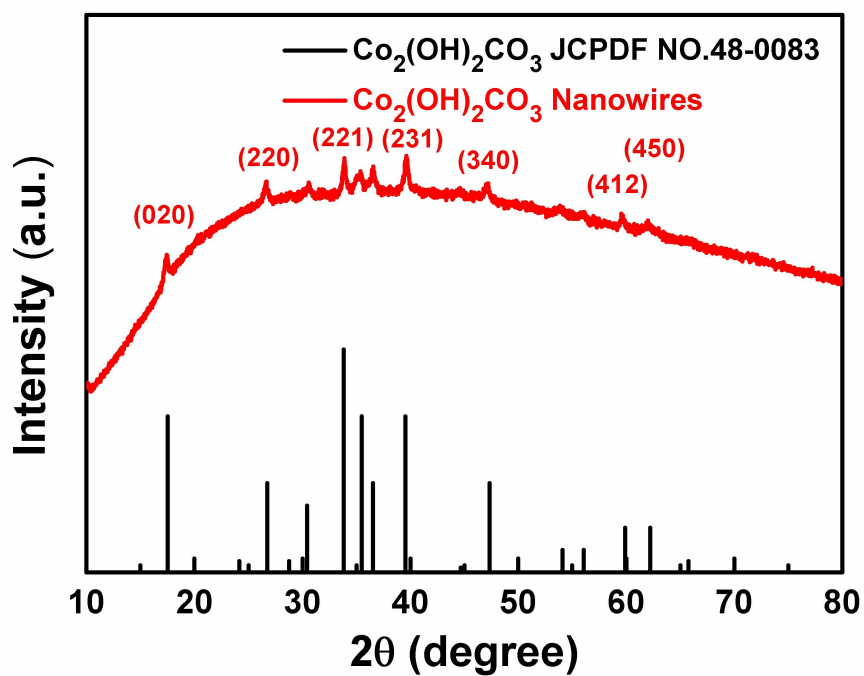**Figure S2.** XRD pattern $Co_2(OH)_2CO_3$ nanowire precursor.
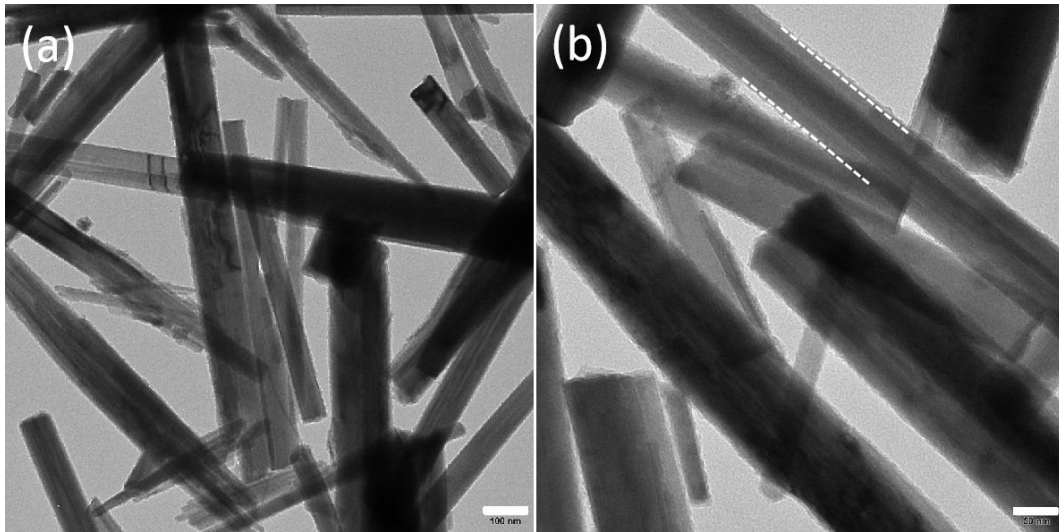
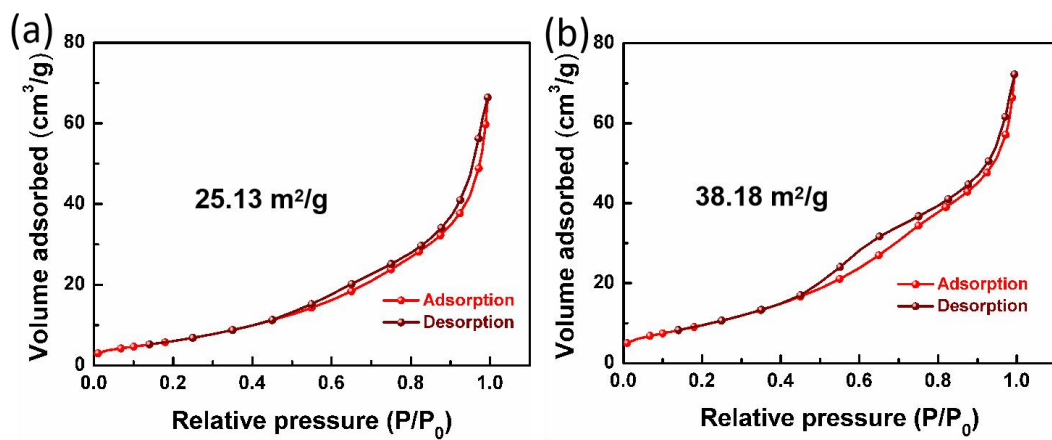**Figure S3.** (a) Low-magnification and (b) high-magnification TEM images of Co$_2$(OH)$_2$CO$_3$@PDA nanowire.

Figure S4. N$_2$ adsorption desorption isotherm curves of (a) Co$_2$(OH)$_2$CO$_3$ nanowire precursor and (b) CoSe$_2$@N-C nanowires.
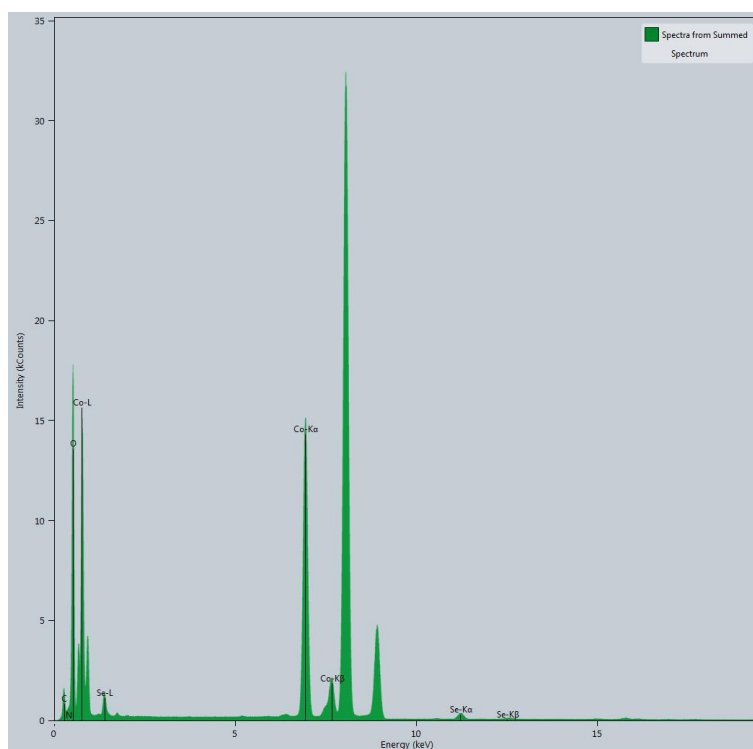
Figure S5. EDX spectrum of CoSe$_2$@N-C nanowires on copper mesh.

Elements	EDS results(%)
Co	39.2
Se	32.3

Figure S6. Atom% of Co and Se in CoSe$_2$@N-C sample.
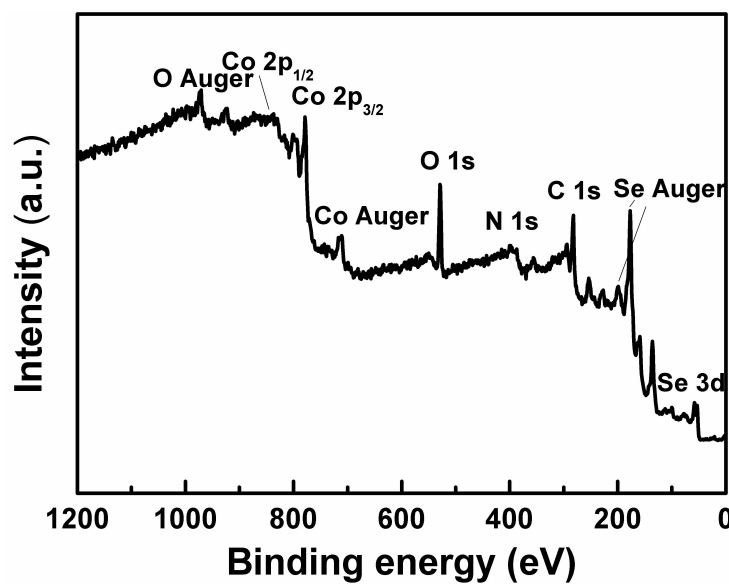
Figure S7. The full XPS spectrum of CoSe₂@N-C nanowires.
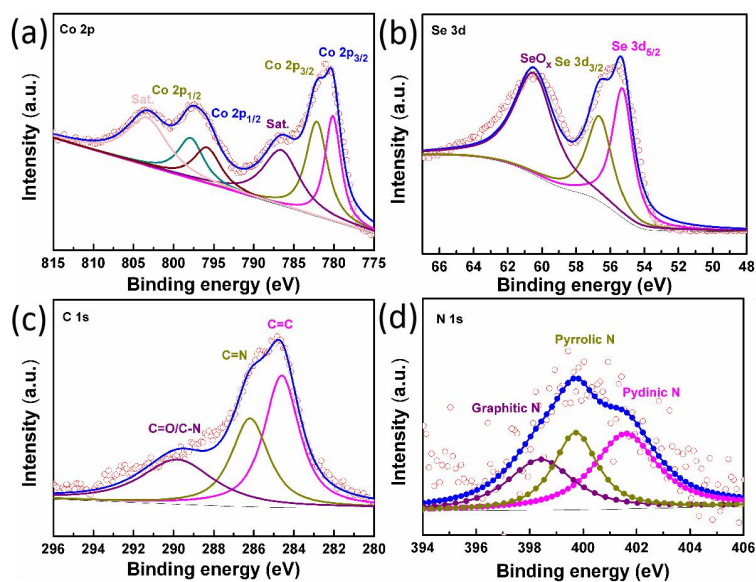
Figure S8: XPS characterization of CoSe₂@N-C NWs. High-resolution XPS spectra of (a) Co 2p. (b) Se 3d. (c) C 1s. (d) N 1s.
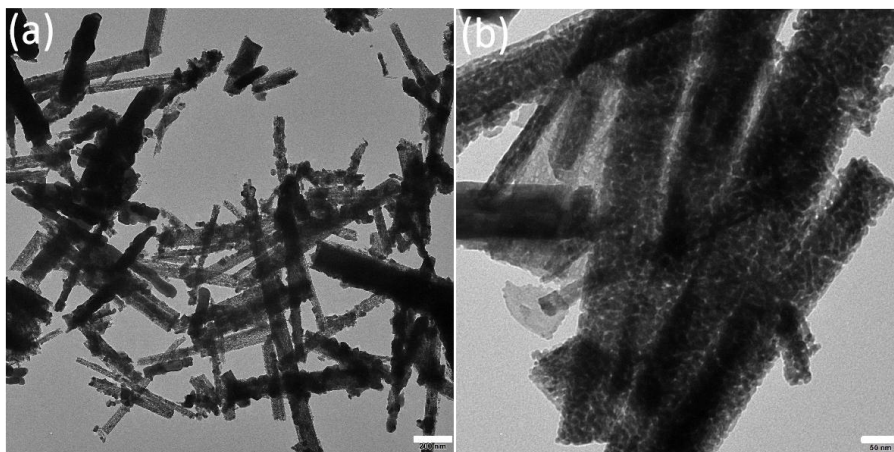
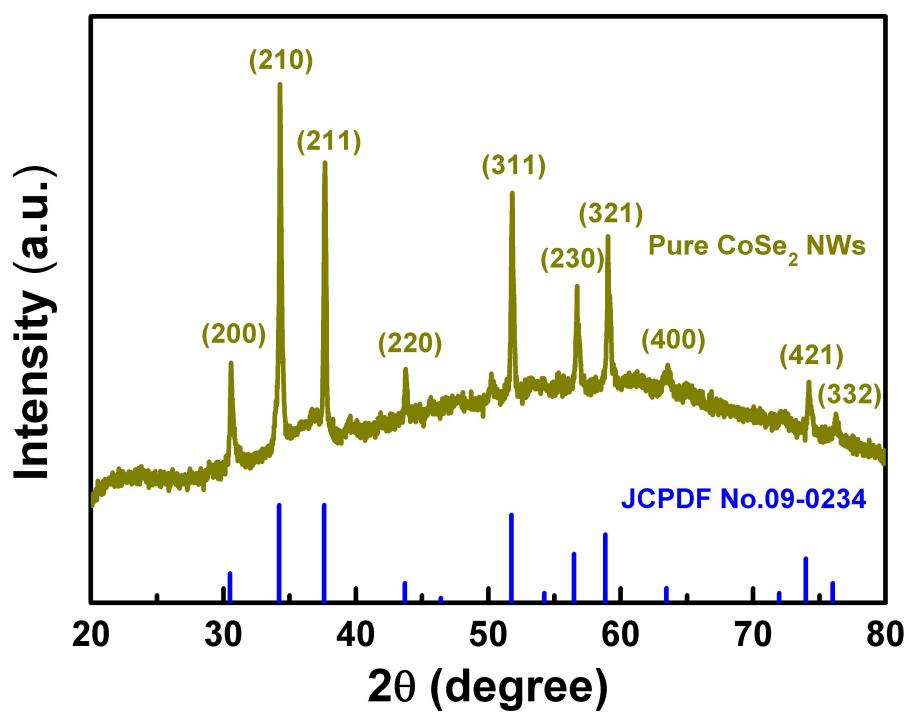**Figure S9.** The TEM image of as-prepared pure CoSe₂ nanowires.

Figure S10. The XRD pattern of as-prepared pure CoSe₂ nanowires.
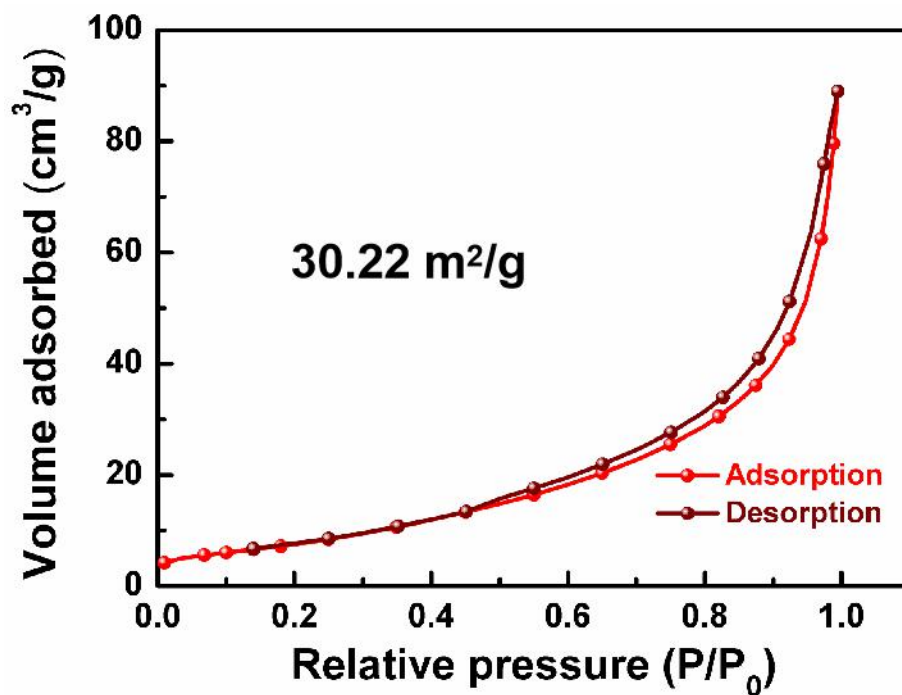
Figure S11. N$_2$ adsorption desorption isotherm curves of as-prepared pure CoSe$_2$ nanowires.
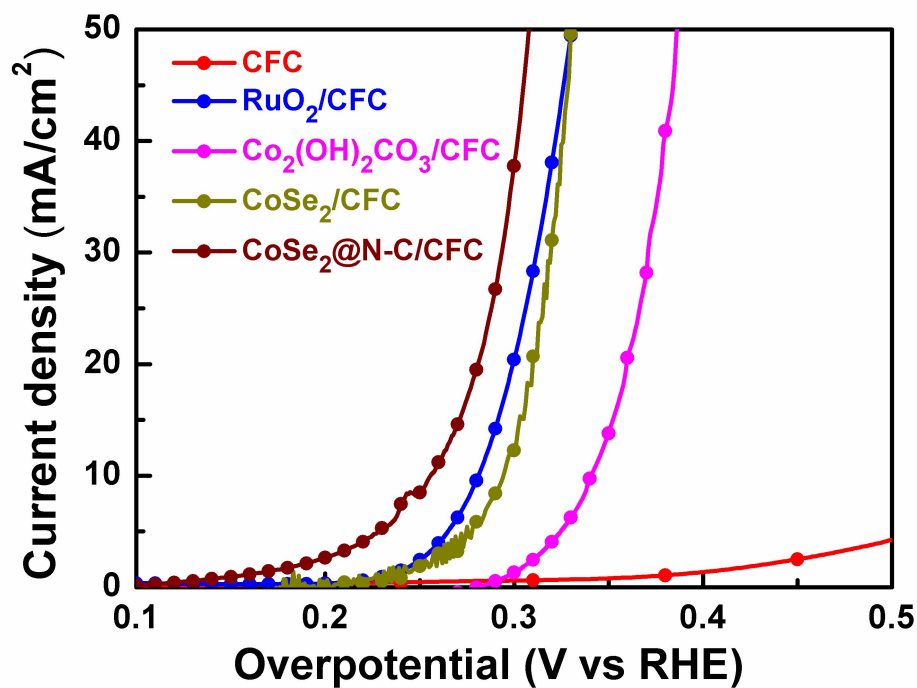

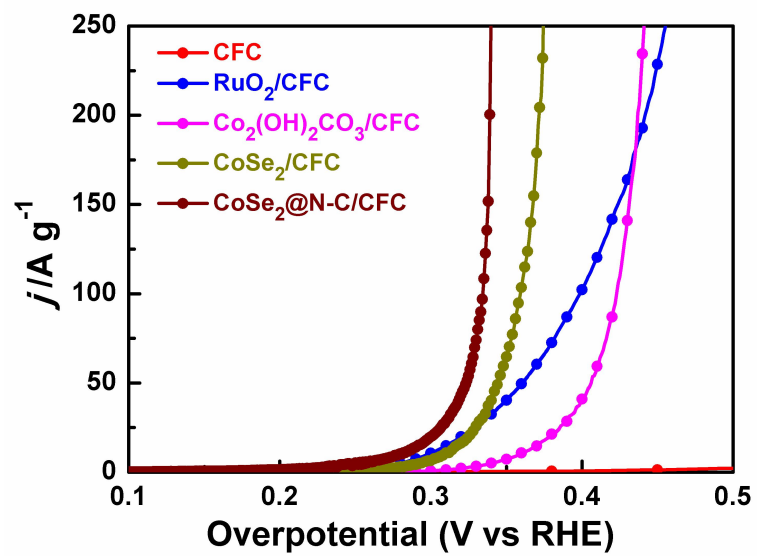**Figure S12.** The enlarged OER polarization curves.

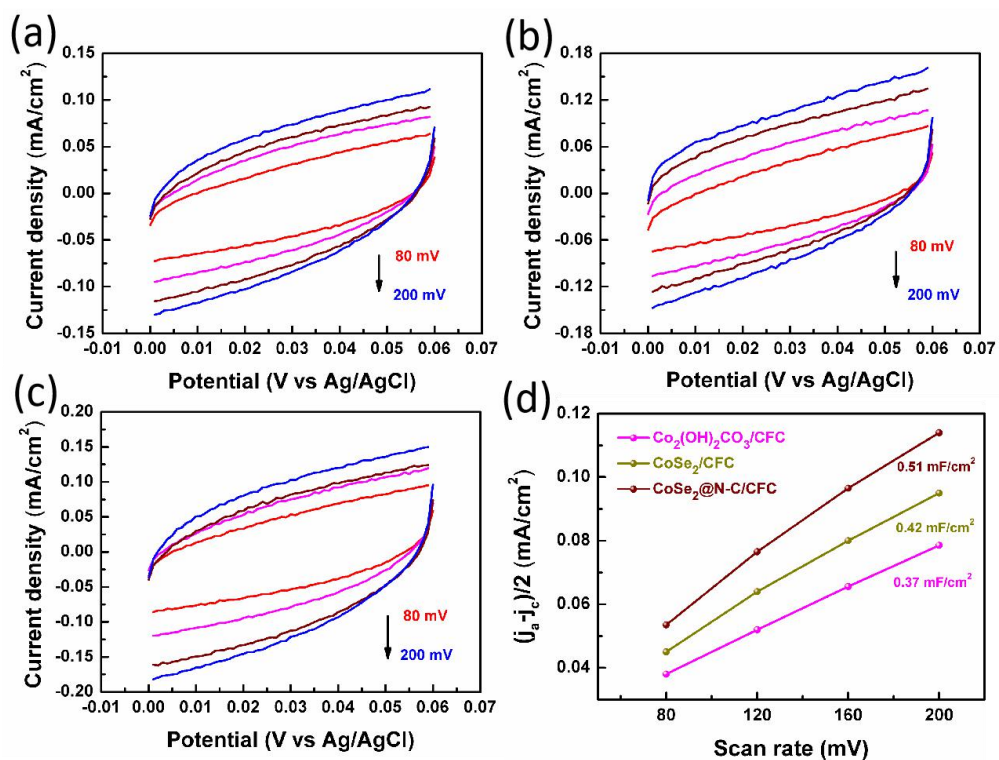**Figure S13.** OER polarization curves normalized by the load capacity.

Figure S14. Electrochemical double-layer capacitance measurements at different scan rates for HER. Cyclic voltammograms of (a) $Co_2(OH)_2CO_3$ NWs/CFC, (b) pure $CoSe_2$ NWs/CFC and (c) $CoSe_2$@N-C NWs/CFC. (d) Capacitive currents with various scan rates. The current density differences (ja-jc) at the open circuit potential plotted against the scan rate.
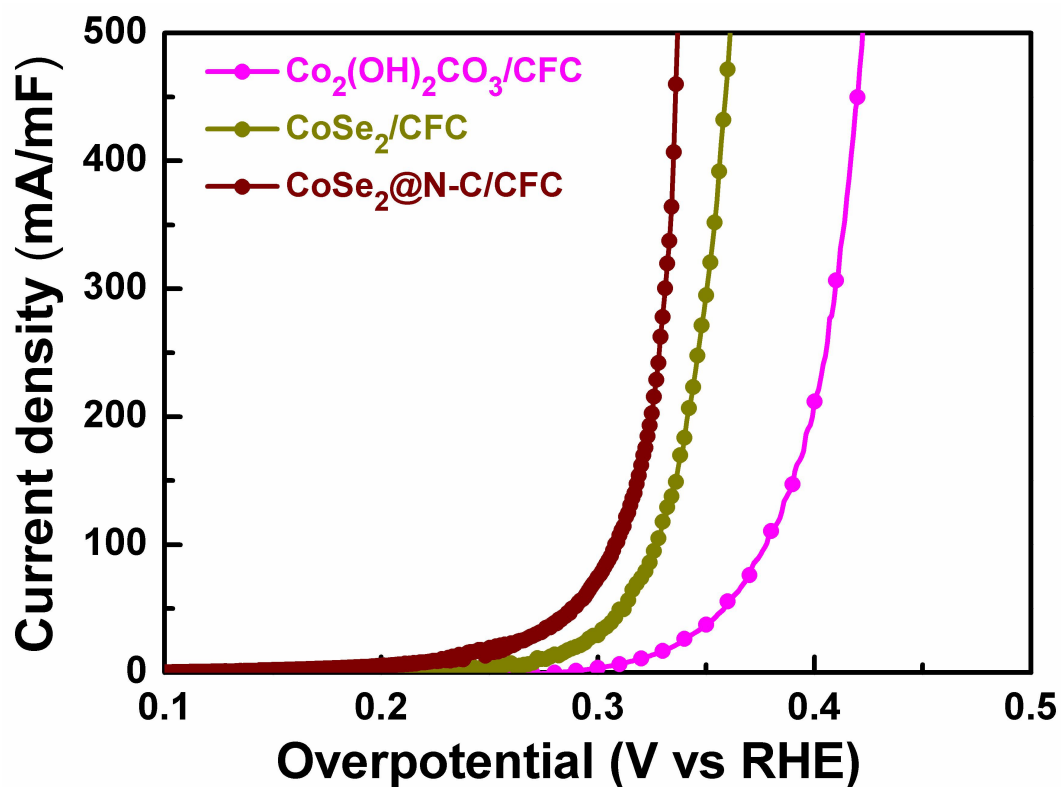
Figure S15. OER polarization curves normalized by the electrochemical double-layer capacitance. The normalized current density of the $CoSe_2$@N-C NWs/CFC is still obviously larger than those of other samples, implying its higher intrinsic activity that the $CoSe_2$@N-C NWs/CFC possess a higher intrinsic electrocatalytic activity than that of other control samples.
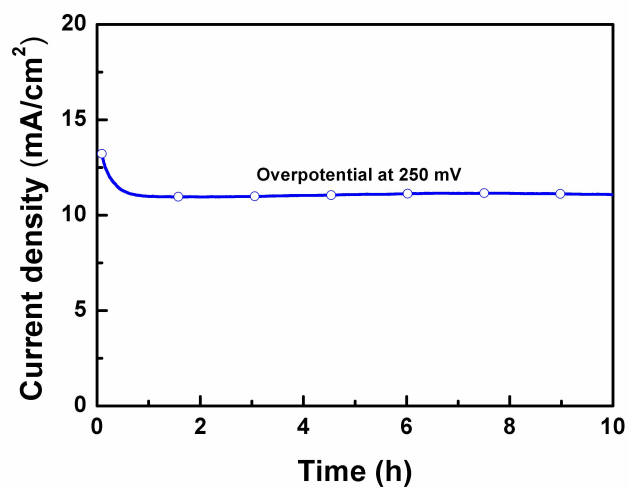
Figure S16. The enlarged i-t curves at the beginning region.

Notes for Figure S16:

At the very beginning, the large activity drop from the first data point to the second activity dropped from 13 to 11 mA/cm^2 are caused by two reasons:

(i) At the test beginning, the electrode have a capacitor release process, this process may lead the activity rapid decrease;

(ii) In addition, at the test beginning, the electrode have a electrolyte permeates and surface stabilization process, this process also will lead the activity rapid decrease.
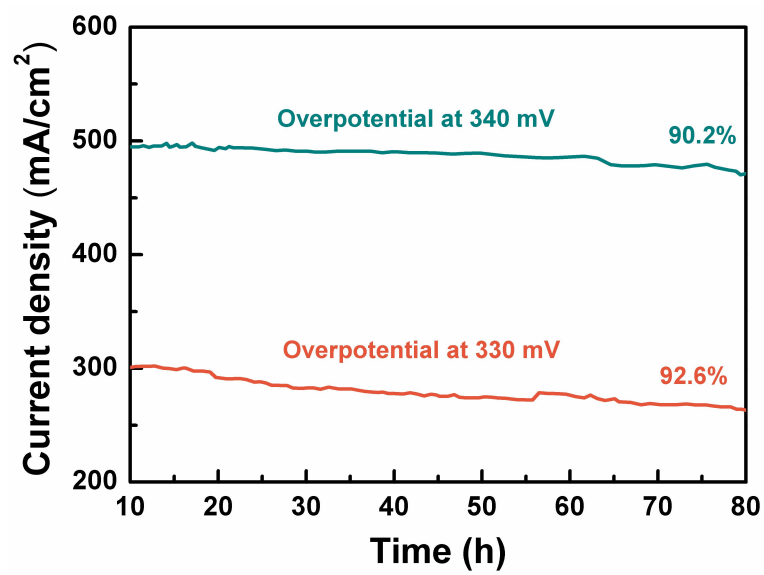
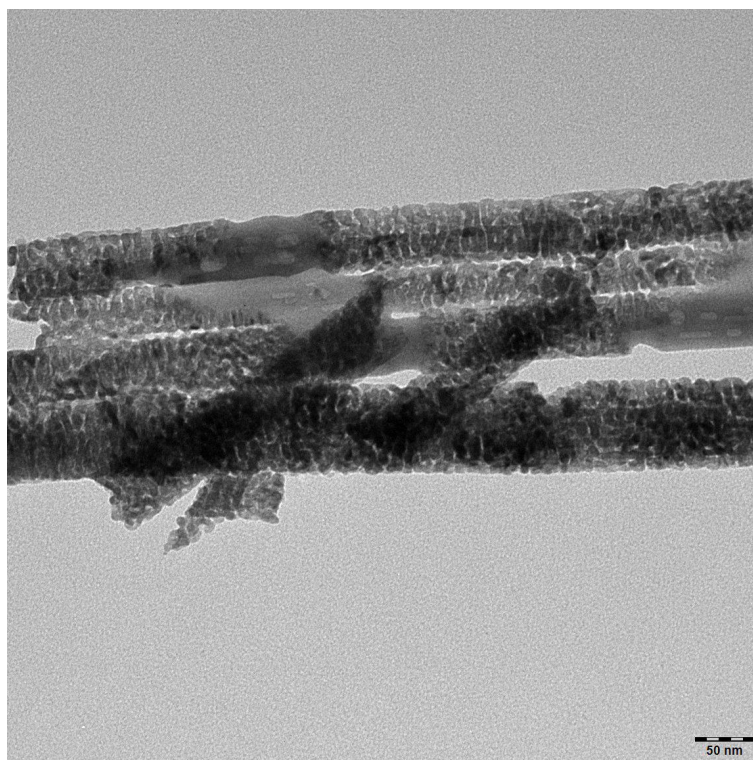**Figure S17.** I-t curves at high current density (300 mA/cm^2 and 500 mA/cm^2).
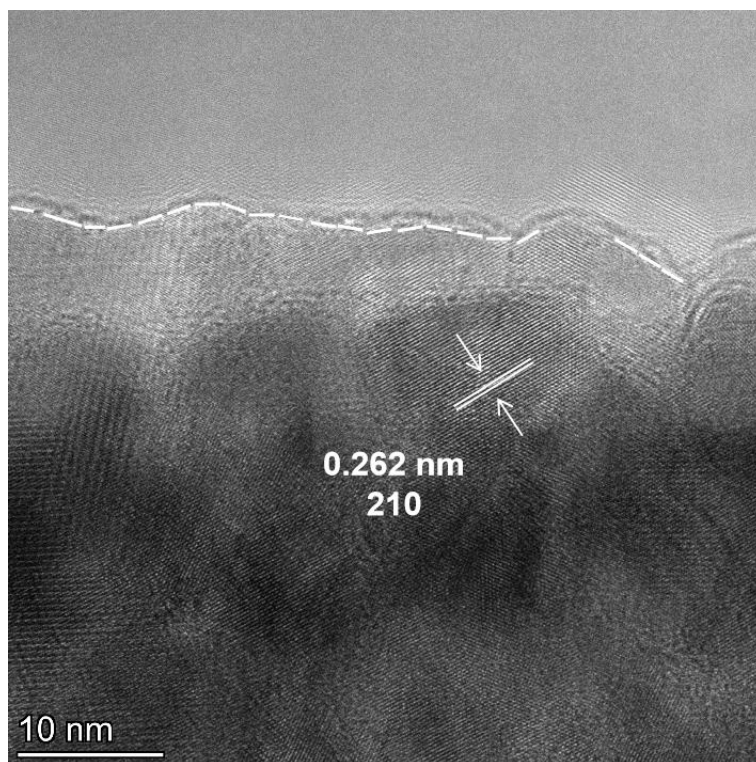

Figure S18. The TEM image of CoSe$_2$@N-C NWs after OER test.

Figure S19. The HRTEM image of CoSe$_2$@N-C NWs after OER test.